fibers

MDPI

Article

Study on Dry Shrinkage Cracking and Shear Strength of Expansive Soils Synergistically Improved with Biochar and Sisal Fibers

Long Ling, Aijun Chen, Yifan Zhou and Yanping Liu *

School of Architecture and Transportation Engineering, Guilin University of Electronic Technology, Guilin 541004, China

* Correspondence: lypdora@guet.edu.cn

Highlights

What are the main findings?

- Adding 10% biochar alone reduced the crack ratio of expansive soil by 86.8% and increased the internal friction angle from 14.84° to 18.52°; adding 6‰ sisal fiber alone increased cohesion from 4.7 kPa to 50.3 kPa, a 970% increase.
- Under combined addition, biochar content had the greatest effect on crack ratio and crack length, while fiber content had the greatest effect on crack width. At 10% biochar, 4.5‰ sisal fiber, and 20 mm fiber length, no cracks formed on the soil surface.

What are the implications of the main findings?

- At the optimal mix ratio, the treated soil developed no surface cracks. Its cohesion, internal friction angle, and crack ratio can be adjusted by varying the biochar and sisal fiber contents and fiber length.
- This method uses agricultural/forestry waste and natural plant fiber to replace cement or lime, suppressing cracks while reducing carbon emissions from material production.

Abstract

Expansive soil is highly susceptible to water-softening and desiccation cracking under alternating wet–dry conditions, often resulting in severe geotechnical and geological hazards. To mitigate these undesirable engineering properties, a composite improvement approach utilizing biochar and sisal fiber was employed. The shear strength and cracking characteristics of the improved expansive soil were systematically investigated through direct shear tests and desiccation cracking tests on specimens prepared with varying biochar contents, sisal fiber contents, and fiber lengths. Scanning electron microscopy (SEM) was further conducted to elucidate the underlying microstructural mechanisms. The results indicated that the individual addition of biochar or sisal fiber enhanced the shear strength of the expansive soil. Increasing the biochar content from 4% to 10% yielded an 8–19% strength gain, whereas raising the sisal fiber content from 1.5‰ to 6‰ led to a more substantial 36–110% improvement. Conversely, extending the fiber length from 10 mm to 30 mm diminished the shear strength by 11–21%. Higher biochar contents progressively increased the internal friction angle (from 14.84° to 18.52°) but were accompanied by a decline in cohesion (from 9.0 kPa to 4.0 kPa). In contrast, increasing the sisal fiber content markedly enhanced cohesion (from 4.7 kPa to 50.3 kPa) while marginally reducing the internal friction angle (from 15.2° to 12.8°). In terms of crack suppression, a 10% biochar content achieved an 86.8% reduction in crack ratio, while 6‰ sisal fiber yielded a 72.4% reduction. Range analysis revealed that crack length and crack ratio were most sensitive to biochar content,

Check for updates

Academic Editors: Martin J. D. Clift and Sushanta Ghoshal

Received: 10 May 2026
Revised: 1 July 2026
Accepted: 7 July 2026
Published: 13 July 2026

Copyright: © 2026 by the authors. Licensee MDPI, Basel, Switzerland. This article is an open access article distributed under the terms and conditions of the Creative Commons Attribution (CC BY) license.

whereas crack width was predominantly governed by fiber content. Notably, surface cracking was completely eliminated in the composite specimen prepared with 10% biochar, 4.5‰ sisal fiber, and a fiber length of 20 mm. Microstructural analysis revealed that biochar particles featured rough surfaces and abundant internal pores, while the sisal fibers formed a randomly interwoven network within the soil matrix. The synergistic interplay between the rigid biochar skeleton and the flexible fiber network contributed to the substantial enhancement in both mechanical strength and crack resistance.

Keywords: expansive soils; biochar; sisal fiber; direct shear test; fracture indicators

1. Introduction

Expansive soil is a highly plastic clay characterized by poor water stability, pronounced swell–shrink behavior, and a high susceptibility to desiccation cracking. Alternating wet and dry seasons induce cyclic swell–shrink deformation, strength degradation, and crack propagation, which can readily lead to engineering distresses such as pavement corrugation and fracturing, as well as cracking of building walls. The persistent and recurrent nature of these problems causes substantial economic losses [1–3]. Recent studies have revealed that under extreme drought conditions, crack evolution in expansive soil embankments progresses through three distinct stages—slow, rapid, and steady development—with crack intensity at the embankment crest being two to three times that on the upstream and downstream slopes [4]. A size effect has also been identified in soil desiccation cracking, with cracking behavior tending to stabilize once the dimensionless size parameter λ exceeds 9.0 [5]. Furthermore, desiccation cracks can drastically alter the internal moisture distribution, increasing pavement edge settlement by as much as 300% [6]. These findings elucidate the complex cracking mechanisms of expansive soils under wetting–drying cycles and highlight the urgent need for sustainable improvement strategies. Among the emerging sustainable materials, biochar has proven effective in stabilizing vegetated expansive soil slopes by modulating hydrothermal properties [7], and its combination with natural fibers has demonstrated synergistic potential for suppressing swell–shrink behavior [8,9]. Nevertheless, the adoption of environmentally friendly and cost-effective methods to enhance expansive soil strength while suppressing cracking remains a critical challenge in geotechnical engineering. While traditional cement- and lime-based stabilization is increasingly discouraged due to its high carbon footprint and adverse ecological impacts, bio-based alternatives such as biochar and sisal fiber have emerged as promising and sustainable solutions.

Biochar is produced from plant materials or animal manure through pyrolysis and gasification under high-temperature, oxygen-limited conditions [10–14]. Previous studies have demonstrated that plant-based biochar [15], when applied at a high content (10%) under high-density compaction, can effectively reduce the evaporation rate and thereby control crack development. For instance, corn straw biochar [16] suppresses cracking in expansive soils primarily by delaying soil moisture evaporation and enhancing aggregate integrity, reducing the crack ratio by 32.39% and 15.31% at contents of 4% and 8%, respectively. Woody biochar [17] can decrease the surface crack ratio of silty clay by approximately 50% and the crack width by about 40%, with the suppression effect becoming more pronounced after wetting–drying cycles. Wheat straw biochar [18] exhibits optimal crack-suppressing performance at a content of 5%, reducing the surface crack ratio by roughly 30%. Several biochar types [19], including wheat straw biochar (SB), wood chip biochar (WCB), and wastewater sludge biochar (WSB), reduce the coefficient of linear extensibility

(COLE), thereby mitigating surface crack formation and lowering the surface crack area density. With regard to the effect of biochar on clay strength, Wang et al. [20] reported that 5% straw biochar increased the cohesion and internal friction angle of expansive soil by 20% and 5°, respectively, after five wetting–drying cycles. Shailesh et al. [21] found that 2% bamboo biochar enhanced the unconfined compressive strength (UCS) of silty clay by 10.51%, whereas at contents of 3.5% and 5%, the UCS decreased by 12.92% and 24.29%, respectively, relative to the unamended soil. Although these studies confirm that biochar can inhibit crack development in clay soils, its effects on clay strength remain insufficiently understood.

Fiber materials, including both synthetic and natural types, have been widely used to enhance soil strength and inhibit crack development. For instance, straw fiber [22] exhibited optimal crack resistance at a content of 0.3% after 25 days of wetting–drying cycles, with a clay surface shrinkage ratio of 10.31%. Sisal fiber-reinforced expansive soil [23] showed a reduction in crack ratio and mean crack width by up to approximately one-half compared with unreinforced soil at a fiber content of 0.4% and a length of 20 mm. Polyester fiber [24] reduced the crack intensity factor of expansive clay by 66%, with the most effective suppression achieved at a content of 0.5% and a length of 15 mm. Although flax fiber [25] had little influence on the initial crack development of kaolin, it reduced the crack ratio by approximately eightfold (i.e., an 87.5% reduction). Polypropylene fiber [26] decreased the crack ratio of clay by roughly 40% at a content of 0.8%, with fiber length (6–19 mm) showing no significant influence on the crack-suppressing effect. Similar findings were reported by Huang et al. [27], Su et al. [28], and Han et al. [29]. In addition to crack suppression, fibers can also improve soil strength. The combined incorporation of polypropylene fiber and sodium silicate [30] significantly enhanced both the unconfined compressive strength and the shear strength of expansive soil. Basalt fiber [31] markedly increased the cohesion of weakly expansive soil, with a certain degree of improvement in shear strength. Both glass fiber and polypropylene fiber [32] enhanced the shear behavior of expansive soil, with polypropylene fiber achieving its peak shear strength at a content of 0.5% and exhibiting a superior crack-suppressing effect compared with glass fiber.

The foregoing analysis indicates that while both biochar and fibers can independently inhibit crack development in soils, and fibers additionally enhance soil strength, their combined application remains largely unexplored. Although a limited number of studies have investigated fibers in conjunction with other materials [30,31], the synergistic mechanisms by which biochar and sisal fiber jointly suppress desiccation cracking and improve shear strength are still poorly understood. Systematic investigations that simultaneously examine the coupled effects of content and length on both strength and cracking are lacking, and the relationship between microstructural characteristics and macroscopic performance has not been adequately elucidated. To address these gaps, this study presents three novel contributions: ① the first application of woody biochar combined with sisal fiber for expansive soil improvement; ② orthogonal tests designed to systematically evaluate the coupled effects of content and length on both mechanical strength and crack behavior; and ③ integration of macroscopic mechanical testing with SEM microstructural observations to reveal the underlying synergistic mechanisms. Specifically, a series of direct shear tests and desiccation cracking tests were conducted to investigate the influence of biochar content, fiber content, and fiber length on the shear strength and crack characteristics of the improved soil. Orthogonal tests were employed to identify the relative significance of each influencing factor and to determine the optimal combination. SEM observations were then used to elucidate the synergistic improvement mechanisms at the microstructural level. The findings are expected to provide a theoretical basis for the prevention and mitigation of expansive soil-related engineering hazards. Furthermore, the use of

agricultural/forestry waste (biochar) and natural plant fibers (sisal fiber) aligns with the United Nations Sustainable Development Goals (SDGs), particularly Goal 9 (Industry, Innovation and Infrastructure), Goal 11 (Sustainable Cities and Communities), and Goal 12 (Responsible Consumption and Production).

2. Materials and Methods

2.1. Materials

The test materials used in this study—expansive soil, sisal fiber, and biochar—are shown in Figure 1. The expansive soil was sampled from a new road construction project in Nanning, Guangxi Zhuang Autonomous Region, China, at a depth of 2.5–4.0 m below the ground surface; the soil exhibited a grayish-green color. The sisal fiber was further processed from raw Guangxi sisal, with an average diameter of 0.12 mm, an elongation at break of 2.1%, an average tensile strength of 564.39 MPa, and an average tensile modulus of 26.97 GPa.The sisal fiber was supplied by Nanning Naizhelu Fiber Products Co., Ltd. (Nanning, Guangxi, China). The biochar was a wood-derived biochar produced from waste wood through high-temperature carbonization and combustion. Prior to use, it was milled and passed through a 2 mm sieve. The biochar had a pH value of 9.17 and a specific surface area of 209.14 m^2/g.The biochar was obtained from Guilin Tanbao Bioenergy Technology Co., Ltd. (Guilin, Guangxi, China).



(**a**) (**b**) (**c**)

Figure 1. Testing material. (**a**) Expansive soil; (**b**) Sisal fiber; (**c**) Biochar.

The basic physical properties of the expansive soil are summarized in Table 1, and the particle size distribution curve obtained from the particle analysis test is presented in Figure 2. The liquid limit (LL) and plastic limit (PL) of the soil were 42.7% and 16.5%, respectively, and the free swell ratio was 55%, indicating weak expansibility based on preliminary classification. According to the Chinese Geotechnical Test Code, soils with a fine-grained fraction (particle size < 0.075 mm) accounting for 50% or more of the total mass are classified as low-liquid-limit clay.

Table 1. Basic physical properties of expansive soils.

Shrinkage Limit ω_s (%)	Plastic Limit ω_p (%)	Liquid Limit ω_l (%)	Plasticity Index I_p (%)	Specific Gravity	Optimum Moisture Content ω_{opt} (%)	Maximum Dry Density ρ_{dmax} (g/cm)	Free Swelling Ratio (%)
13.4	16.5	42.7	26.2	2.71	11.40	1.960	55

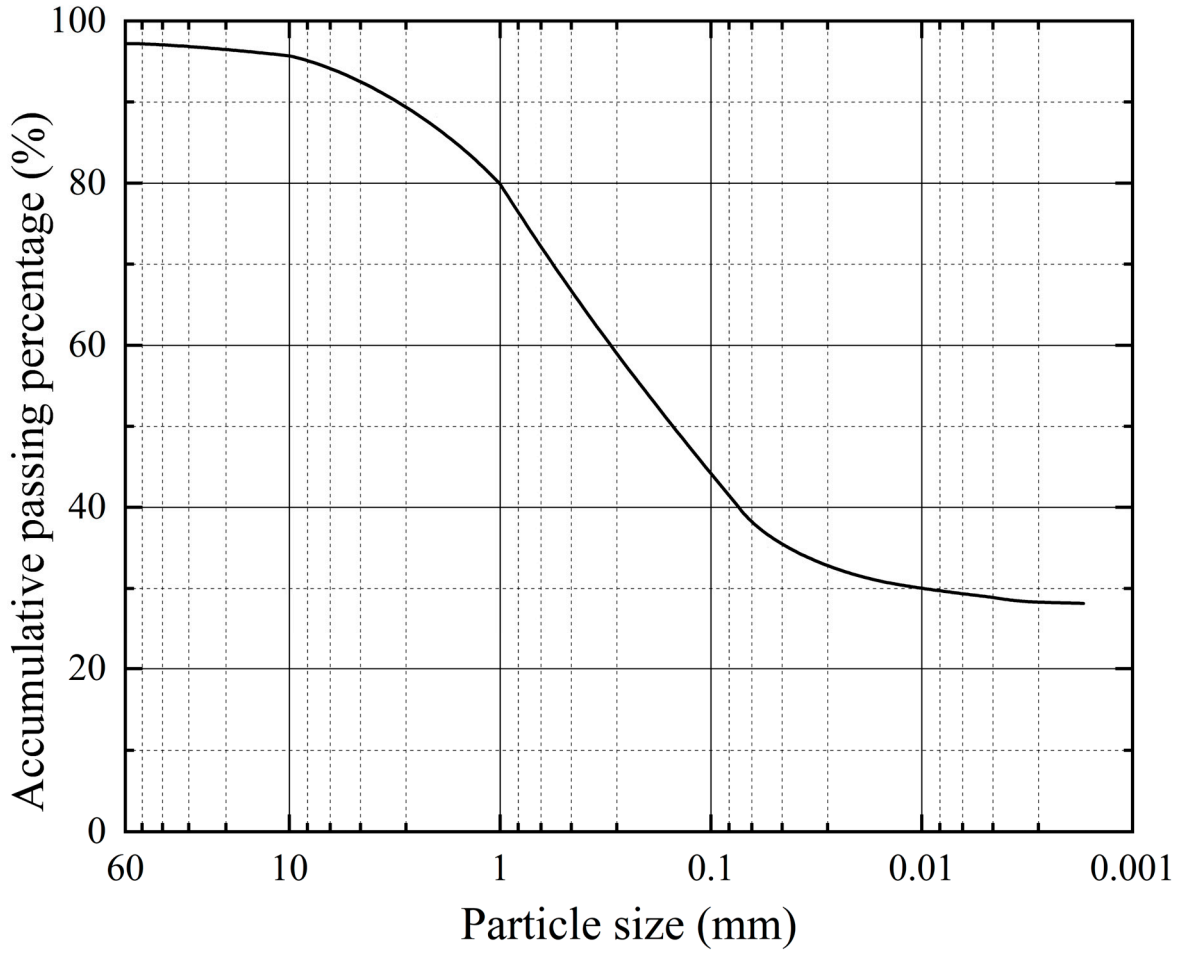


Figure 2. Expanded soil particle grading curve.

2.2. Specimen Preparation

2.2.1. Preparation of Direct Shear Test Specimens

The direct shear test specimen was a ring-shaped specimen with a diameter of 61.8 mm and a height of 20 mm. In accordance with the minimum compaction requirements specified in the Chinese Specifications for Design of Highway Subgrades (JTG D30–2015), the compaction degree of the specimens was set at 94%. The target moisture content of the specimens was determined to be 18%, based on the local subgrade equilibrium moisture content in Guangxi, China. During specimen preparation, air-dried expansive soil (passed through a 2 mm sieve), biochar, and sisal fiber were first mixed in a dry state at the designed proportions (Table 2). The mixing was performed manually using a stainless steel spatula for 10 min until the fibers were uniformly dispersed throughout the soil, with no visible fiber agglomeration upon visual inspection. Deionized water was then uniformly sprayed onto the mixture using a sprayer while stirring continuously to achieve the target moisture content of 18%. After water addition, the mixed soil was sealed in plastic bags and allowed to equilibrate at room temperature (25 ± 2 °C) for 48 h to ensure thorough moisture migration and homogenization. The soil was subsequently compacted into ring-shaped specimens by static compression, stacked in a ring-knife saturator, and subjected to vacuum saturation to obtain fully saturated specimens. The complete test procedure is illustrated in Figure 3.

Table 2. Improved expansive soil direct shear test scheme.

	Biochar Content/%	Sisal Fiber Content/‰	Sisal Fiber Length/mm
i	4, 6, 8, 10	/	/
ii	/	1.5, 3, 4.5, 6	20
iii	/	4.5	10, 20, 30



Figure 3. Preparation of direct shear specimen.

2.2.2. Preparation of Desiccation Cracking Test Specimens

For the desiccation cracking test, the prepared soil mixture was placed into a stainless steel mold measuring 250 mm × 250 mm × 50 mm and evenly leveled. A steel plate was positioned on the surface, and the soil was pre-compacted manually before being statically compacted with a hydraulic press to a final specimen thickness of 15 mm. To facilitate crack identification, a thin layer of flour was uniformly sprinkled onto the specimen surface. The flour was passed through a 0.2 mm aperture sieve from a height of approximately 30 cm, and the sieving was repeated 2–3 times to achieve a flour layer thickness of approximately 0.5 mm. Although the flour absorbed a small amount of water, its influence on the desiccation cracking behavior was considered negligible due to its minimal thickness and fine particle size. The specimen preparation process is illustrated in Figure 4.

2.3. Test Scheme

2.3.1. Direct Shear Test

To investigate the individual effects of biochar and sisal fiber on the strength of expansive soil, a series of single-addition experiments were conducted. Previous studies suggest that the appropriate biochar content is approximately 8%, with the optimal content for agricultural applications being around 10% [15–17,33]. Based on this optimal range (8–10%), two lower contents of 4% and 6% were added to systematically examine the

influence of biochar content across a wider spectrum and to evaluate the improvement effects at lower dosages. Accordingly, the biochar content was set at 4%, 6%, 8%, and 10%.

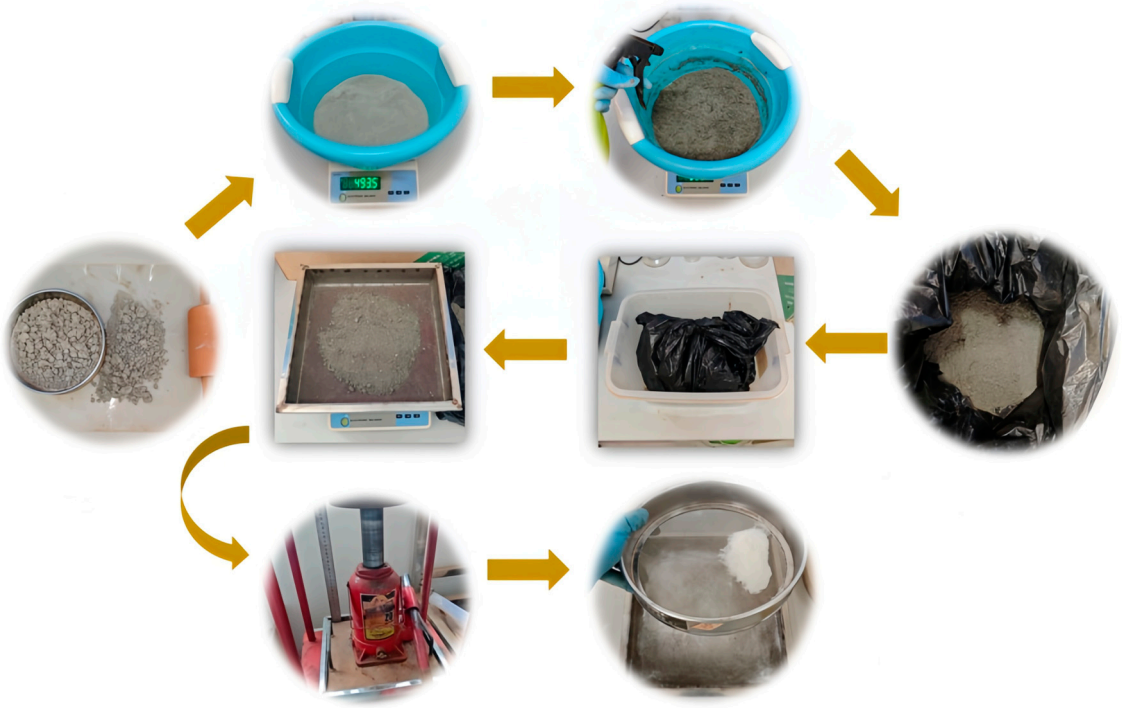


Figure 4. Preparation of desiccation cracking specimen.

For sisal fiber, prior research has indicated an optimal content range of 3–5‰ and a recommended maximum length of 30 mm [22–24]. To comprehensively assess the influence of both content and length, the fiber content was extended downward to 1.5‰ to capture the reinforcement effect at a low dosage and upward to 6‰ to investigate potential performance degradation at high content (i.e., the "over-reinforcement" phenomenon). The fiber contents were thus established as 1.5‰, 3‰, 4.5‰, and 6‰, with fiber lengths of 10 mm, 20 mm, and 30 mm. The complete experimental scheme is summarized in Table 2.

The direct shear tests were performed using the consolidated quick shear method. Under each applied normal pressure, the specimen was first fully consolidated and drained. Once the pore water pressure had dissipated and the specimen had attained a stable consolidated state, the shear stress was applied rapidly at a shear rate of 0.02 mm/min. Shearing was terminated at a shear displacement of 4 mm when a distinct peak shear stress was observed, and at 6 mm when no clear peak appeared. All procedures complied with the relevant provisions of the Chinese Standard for Geotechnical Test Methods (GB/T 50123–2019) [34].

It should be noted that each direct shear test was performed once per group in this study. Although replicate tests were not conducted to calculate standard deviations, the observed trends in strength variation (see Figures 4–6) exhibited clear monotonic regularity and were consistent with those reported in the literature [32,35]. Therefore, the results presented herein should be interpreted as representative trends rather than statistically derived mean values.

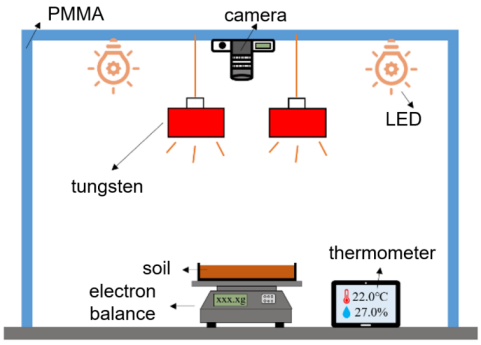


Figure 5. Drying device.

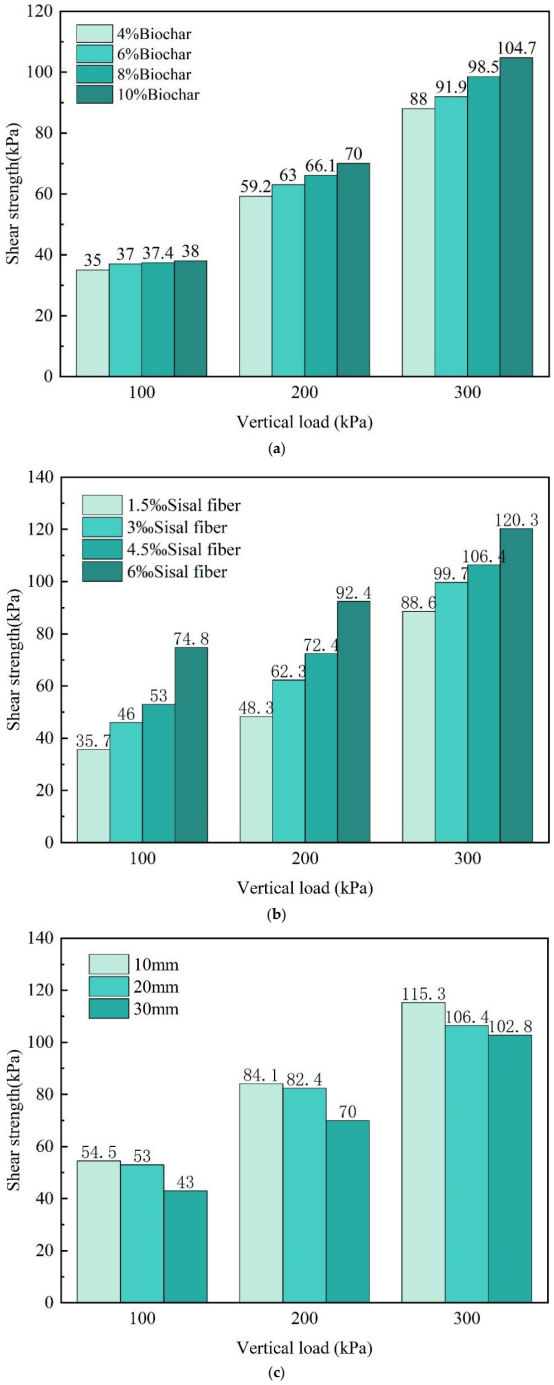


Figure 6. Shear strength of improved soil. (**a**) Biochar content; (**b**) Sisal fiber content; (**c**) Sisal fiber length.

2.3.2. Desiccation Cracking Test

To examine the influence of biochar content, sisal fiber content, and fiber length on the desiccation cracking behavior of expansive soil, the experimental program was designed as summarized in Table 3, and the custom-built drying apparatus is shown in Figure 5. All drying tests were conducted under controlled environmental conditions at a temperature of 25 ± 1 °C and a relative humidity of 30 ± 2%. Specimen mass and crack development were simultaneously monitored using a balance and a digital camera, with images captured at 10-min intervals. The test was considered complete when the change in specimen mass remained below 0.5 g over a 30-min period.

Table 3. Dry shrinkage cracking test scheme.

	Biochar Content/%	Sisal Fiber Content/‰	Sisal Fiber Length/mm
(i)	/	/	/
(ii)	4, 6, 8, 10	/	/
(iii)	/	1.5, 3, 4.5, 6	20

Crack images were processed using Matlab (Matlab 2022A) according to the following procedure: (1) RGB images captured by the camera were converted into grayscale images; (2) Otsu's thresholding method was applied for binarization segmentation to separate the cracks (black) from the soil matrix (white); (3) dilation and erosion operations were performed to remove noise; (4) the Zhang–Suen algorithm was employed to extract the crack skeleton; and (5) spurs shorter than 2 mm were eliminated. The crack ratio was defined as the percentage of black pixels relative to the total pixels in the binary image. The crack length was determined as the total length of all skeleton pixels in the skeleton image (unit: mm, calibrated using a calibration plate). The crack width was calculated by dividing the crack area by the skeleton length. The image processing resolution was 0.05 mm/pixel, and the measurement error was controlled within ±2%.

In this study, each desiccation cracking test was performed once per group. The crack characteristic parameters (crack ratio, length, and width) were automatically extracted using a Matlab image processing program, thereby minimizing human error. Although replicate tests were not conducted, the variation trends of the crack parameters with content were monotonic and well-defined, demonstrating good regularity in the experimental results. Future studies should incorporate an increased number of replicates to enable robust statistical analysis.

3. Results and Analysis

3.1. Direct Shear Test Results

3.1.1. Influence of Biochar Content on Shear Strength

Figure 6a presents the relationship between the shear strength of biochar-amended expansive soil and biochar content under three different vertical pressures. The shear strength increased progressively with biochar content, and this enhancement was more pronounced at higher vertical pressures. Compared with the soil amended with 4% biochar, the shear strength at 10% biochar increased by 8%, 18%, and 19% under the three applied vertical pressures, respectively. Liu et al. [35] reported that for low-liquid-limit clay amended with biochar, the shear strength at a biochar content of 10% was 12% higher than that at 5% under a vertical pressure of 200 kPa. In contrast, Shukla et al. [36] found that incorporating 2% and 4% biochar into fine sand resulted in negligible changes in cohesion, internal friction angle, and shear strength. These findings suggest that the effect of biochar on the shear strength of soils is soil-type dependent: biochar can significantly enhance the shear strength of cohesive soils, whereas it has no appreciable effect on granular soils.

3.1.2. Influence of Sisal Fiber Content on Shear Strength

Figure 6b presents the shear strength of expansive soil amended with sisal fiber at a fixed fiber length of 20 mm. The shear strength increased with increasing fiber content. Under a vertical pressure of 200 kPa, the shear strength at a fiber content of 6‰ was 91% higher than that at 1.5‰. Under vertical pressures of 100 kPa, 200 kPa, and 300 kPa, the shear strength at 6‰ exceeded that at 1.5‰ by 110%, 91%, and 36%, respectively. Notably, the percentage increase in shear strength with fiber content diminished progressively as the vertical pressure increased. A comparable trend was reported for glass fiber-reinforced expansive soil [32], where increasing the fiber content from 1‰ to 3‰ led to a 24% increase in shear strength, consistent with the findings of the present study.

3.1.3. Influence of Sisal Fiber Length on Shear Strength

Figure 6c shows the relationship between sisal fiber length and the shear strength of the improved soil at a fixed fiber content of 4.5‰. The shear strength of the expansive soil decreased with increasing fiber length. Under a vertical pressure of 100 kPa, the shear strength of the soil amended with 30 mm fibers was 21% lower than that with 10 mm fibers; the corresponding reductions were 17% and 11% under vertical pressures of 200 kPa and 300 kPa, respectively. Prabakar and Sridhar [37] similarly observed a decrease in shear strength with increasing sisal fiber length, which is consistent with the findings of this study. These results indicate that excessive fiber length is detrimental to the shear strength improvement of soils.

3.1.4. Influence of Biochar Content on Shear Strength Parameters

Figure 7a presents the shear strength parameters of the improved soil at different biochar contents. As the biochar content increased, the internal friction angle of the expansive soil increased progressively, whereas the cohesion decreased gradually. Specifically, when the biochar content was raised from 4% to 10%, the cohesion declined from 9.0 kPa to 4.0 kPa, while the internal friction angle increased from 14.84° to 18.52°. The reduction in cohesion can be attributed to the low intrinsic viscosity of biochar, which, when ground and uniformly dispersed, reduces the contact area between clay minerals. In contrast, biochar particles are characterized by high hardness and irregular shapes, which enhance particle interlocking between soil particles and biochar under applied vertical loads [38,39]. This rigid skeleton effectively hinders the relative displacement of soil particles during shearing, resulting in an increase in the internal friction angle with increasing biochar content.

3.1.5. Influence of Sisal Fiber Content on Shear Strength Parameters

Figure 7b illustrates the relationship between fiber content and the shear strength parameters of the improved soil. Increasing the sisal fiber content significantly enhanced the cohesion of the expansive soil while moderately reducing its internal friction angle. Specifically, as the fiber content increased from 1.5‰ to 6‰, the cohesion rose from 4.7 kPa to 50.3 kPa, representing a substantial increase of 970%, whereas the internal friction angle decreased from 15.2° to 12.8°, a reduction of 15.2%. The slight decrease in the internal friction angle can be attributed to the fibers occupying the contact space between soil particles, thereby weakening the direct interlocking and friction between them [40]. Conversely, the sisal fibers formed an interwoven three-dimensional network within the soil matrix, which enhanced the overall integrity of the soil by winding, lapping, and wrapping around soil particles. This spatial reinforcement mechanism was primarily responsible for the dramatic improvement in cohesion.

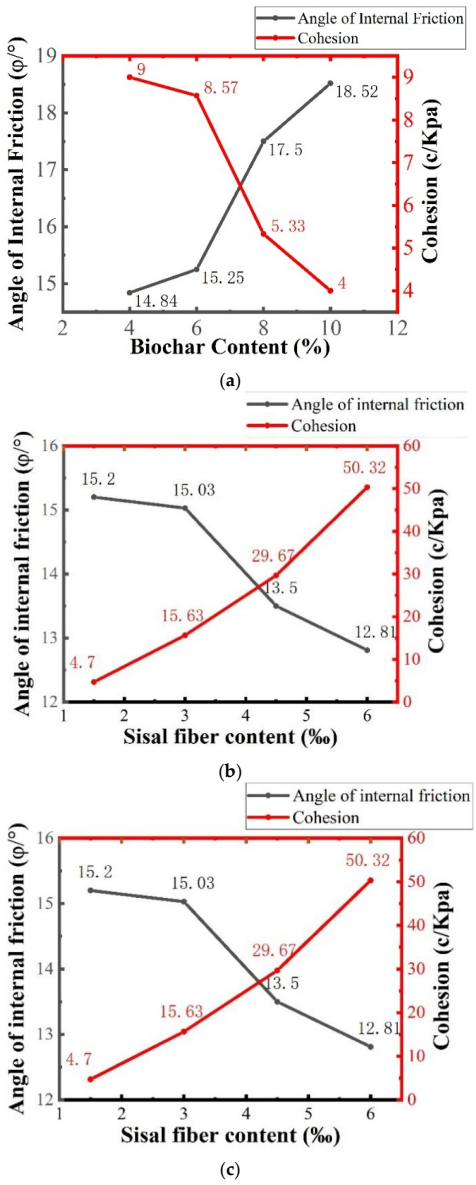


Figure 7. Effect of biochar and sisal fiber on shear resistance index. (**a**) Biochar content; (**b**) Sisal fiber content; (**c**) Sisal fiber length.

3.1.6. Influence of Sisal Fiber Length on Shear Strength Parameters

Figure 7c presents the relationship between sisal fiber length and the shear strength parameters of the improved soil. As the fiber length increased, the cohesion first increased and then decreased, whereas the internal friction angle exhibited an opposite trend, initially decreasing and then increasing. The peak cohesion of 29.7 kPa and the minimum internal friction angle of 13.5° were both attained at a fiber length of 20 mm.

When the sisal fibers are too short, they are unable to form an effective interlocking network; consequently, the reinforcement remains localized, and the improvement in overall cohesion is limited. Conversely, excessively long fibers tend to entangle into clusters [24], leading to a non-uniform distribution that creates fiber-rich and fiber-deficient zones, thereby disrupting the continuity of the soil structure. Consistent with the findings of this study, the greatest cohesion was achieved at a fiber length of 20 mm [37]. This is because 20 mm sisal fibers can be more readily and uniformly dispersed within the soil, forming a continuous three-dimensional network that enhances the mechanical interlocking between soil particles.

The isolation effect provided by 10 mm fibers was relatively weak [40], allowing substantial direct contact between soil particles and resulting in a comparatively high internal friction angle. In contrast, the dense network structure formed by 20 mm fibers effectively separated the soil particles, thereby reducing direct interparticle contact and interlocking, which in turn decreased the sliding resistance (internal friction angle) during shearing. When excessively long fibers were used, their tendency to distribute unevenly or form clusters prevented complete isolation of interparticle occlusion in localized regions; consequently, the reduction in friction was less pronounced, and the internal friction angle increased.

3.2. Desiccation Cracking Test Results

3.2.1. Influence of Biochar Content on Crack Characteristics

Figure 8 presents the relationships between crack length, crack width, crack ratio, and biochar content for the expansive soil amended with biochar alone. All three crack indicators exhibited a general downward trend with increasing biochar content. Compared with the plain soil, the specimen amended with 4% biochar showed reductions of 16.3% in crack length, 50.1% in crack width, and 58.9% in crack ratio. As the biochar content further increased, the crack width reached its minimum at 8%, while the crack length continued to decrease. At 10% biochar content, the crack ratio was reduced by 86.8% relative to the plain soil. Zhang [41] reported that the addition of 6% biochar to high-liquid-limit soil and low-liquid-limit clay reduced the crack ratio by 22.64% and 30.8%, respectively, compared with the corresponding plain soils. Wang [42] found that incorporating 10% biochar into Xiashu soil and red clay resulted in a 32.2% decrease and an 80.4% increase in crack ratio, respectively. These findings indicate that biochar exerts a significant inhibitory effect on soil desiccation cracking; however, the effectiveness is closely related to the clay content, mineral composition, biochar type, and particle size of the soil. Different biochar types exhibit distinct effects on the cracking behavior of different soil types.

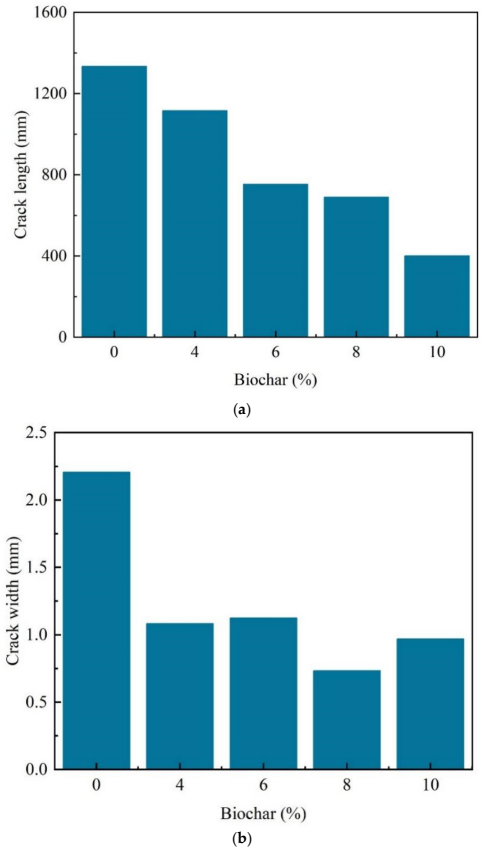


Figure 8. *Cont.*

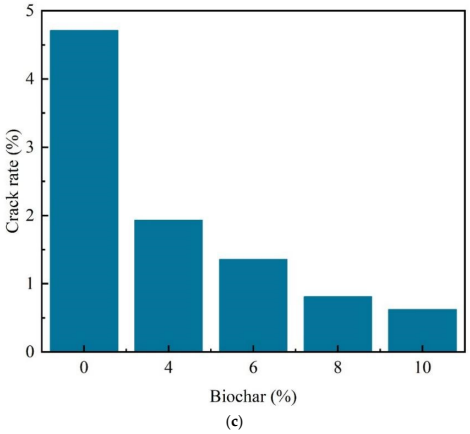


Figure 8. Effect of biochar content on cracks. (**a**) Crack length; (**b**) Crack width; (**c**) Crack rate.

Figure 9 presents a comparison of the surface photographs of the plain soil specimen and the specimen amended with 10% biochar after drying. The images clearly demonstrate that biochar significantly inhibited crack development.

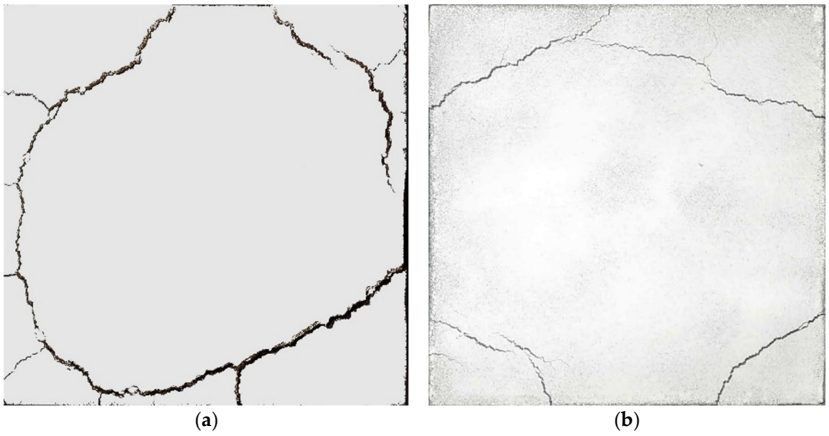


Figure 9. Soil specimens with cracks formed after drying: (**a**) Plain expansive soil and (**b**) expansive soil amended with 8% biochar.

3.2.2. Influence of Sisal Fiber Content on Crack Characteristics

Figure 10 presents the relationships between crack length, crack width, crack ratio, and sisal fiber content for the soil amended with sisal fiber alone at a fixed fiber length of 20 mm. Compared with the plain soil, the specimen amended with 1.5‰ sisal fiber exhibited reductions of 43.7% in crack length, 12.7% in crack width, and 51.1% in crack ratio. With further increases in fiber content, the crack-suppressing effect was progressively enhanced; at a fiber content of 6‰, the crack ratio was merely 27.5% of that of the plain soil. Tang [19] reported a linear decrease in crack ratio with increasing fiber content, noting that the crack ratio of plain expansive soil reached as high as 19.26%, yet remained approximately 11% at a fiber content of 8‰. The crack inhibition effect observed in the present study is considerably more pronounced, with the crack ratio at 6‰ fiber content being only 1.4%. This discrepancy may be primarily attributed to differences in the initial moisture content of the soil specimens and the specimen preparation methods employed.

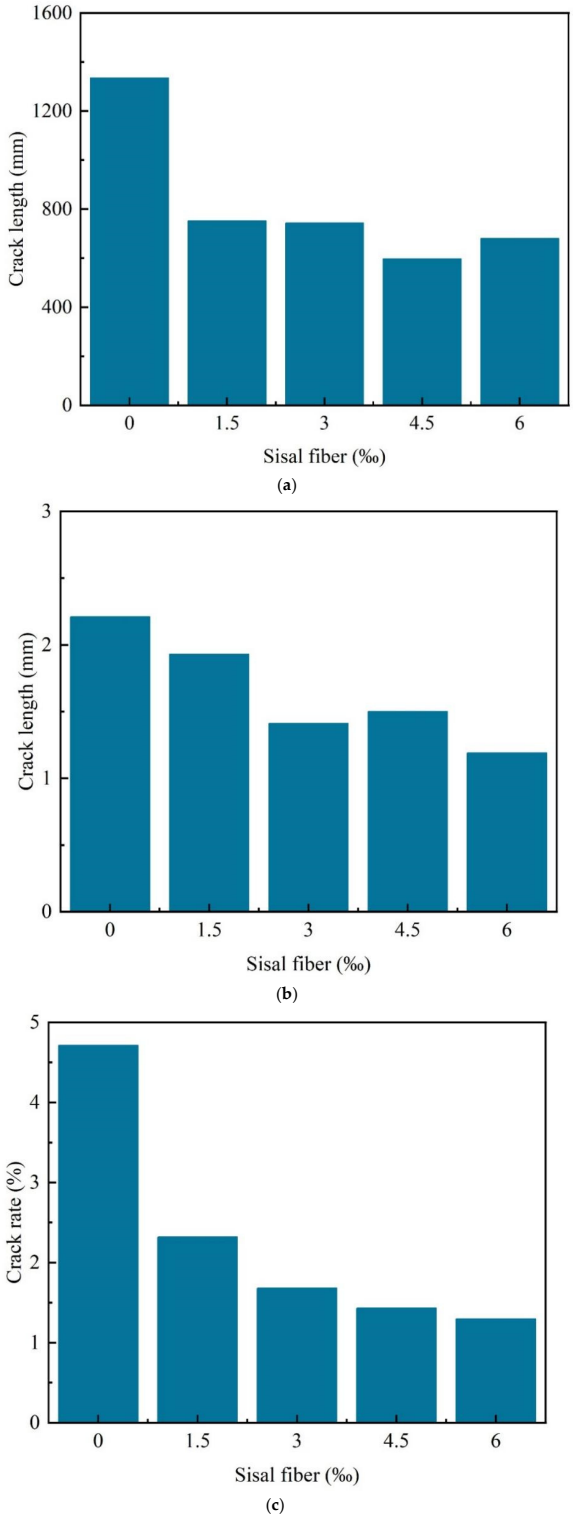


Figure 10. Effect of fiber content on cracks. (**a**) Crack length; (**b**) Crack width; (**c**) Crack rate.

3.2.3. Synergistic Influence Based on Orthogonal Tests

The influence of various factors on the test indicators was evaluated through orthogonal tests, where Factor A represents biochar content (%), Factor B denotes sisal fiber content (‰), and Factor C corresponds to sisal fiber length (mm). The results of the orthogonal test presented in Table 4 were analyzed using range analysis, as summarized in Table 5. In Table 5, K_i represents the mean value of the test indicator at a given level of each influencing factor, with the level corresponding to the maximum K_i identified as the optimal level.

R denotes the range, defined as the difference between the maximum and minimum K_i values for a given factor. A larger R value indicates a more pronounced influence of that factor on the evaluation indicator.

Table 4. Results of orthogonal experiment.

Clusters	A/mm	B/mm	C/mm	Crack Length/mm	Crack Rate/%	Crack Width/mm
1	4	1.5	20	637.67	1.49	1.47
2	4	3	10	488.48	1.06	1.36
3	4	4.5	20	571.86	0.78	0.85
4	4	6	30	500.6	0.24	0.30
5	6	1.5	30	643.86	1.65	1.60
6	6	3	20	496.93	0.43	0.54
7	6	4.5	10	567.85	0.55	0.60
8	6	6	20	339.75	0.22	0.41
9	8	1.5	10	317.97	0.47	0.92
10	8	3	20	277.91	0.17	0.38
11	8	4.5	30	249.38	0.16	0.39
12	8	6	20	116.35	0.19	1.04
13	10	1.5	20	311.71	0.36	0.72
14	10	3	30	441.54	0.51	0.72
15	10	4.5	20	0	0	0
16	10	6	10	488.48	1.06	1.36
17	0	0	0	1334.54	4.71	22.1

Table 5. Results of range analysis for orthogonal experiment.

Index	Mean Value and Range	A	B	C
Crack length/mm	k_1	549.65	477.80	355.22
	k_2	512.10	426.22	474.92
	k_3	240.40	347.27	346.21
	k_4	310.43	399.97	/
	R	309.25	130.53	128.70
Crack rate/%	k_1	0.89	0.99	0.53
	k_2	0.71	0.54	0.68
	k_3	0.25	0.37	0.58
	k_4	0.23	0.43	/
	R	0.66	0.62	0.15
Crack width/mm	k_1	1.00	1.17	0.84
	k_2	0.79	0.75	0.68
	k_3	0.68	0.46	0.75
	k_4	0.48	0.56	/
	R	0.52	0.71	0.16

From Table 5, the R values for crack length followed the order $R_A > R_B > R_C$, indicating that the factors influencing crack length, in descending order of significance, were biochar content > fiber content > fiber length. Comparison of the K_i values under Factor A showed that $K_1 > K_2 > K_4 > K_3$, suggesting that the crack length of the improved soil was minimized when Factor A was at its third level. Similarly, the optimal levels for Factors B and C were also identified as the third level. Therefore, the combination that minimized crack length was A, B, C, corresponding to a biochar content of 8%, a fiber content of 4.5‰, and a fiber length of 30 mm.

Following the same analytical approach, the order of influencing factors for the crack ratio was biochar content > fiber content > fiber length. The combination that minimized the crack ratio was A, B, C, i.e., a biochar content of 10%, a fiber content of 4.5‰, and a fiber length of 10 mm. For the crack width, the influencing factors ranked as fiber

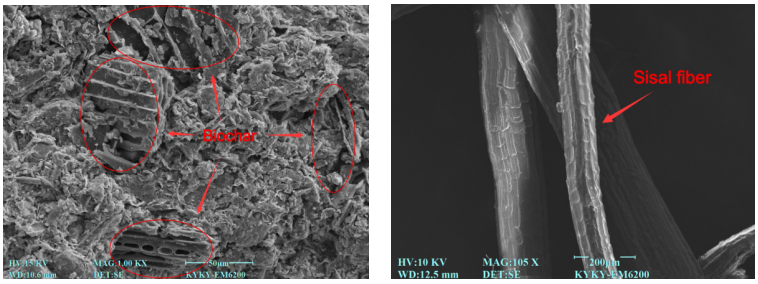
content > biochar content > fiber length, with the minimum crack width achieved at a biochar content of 10%, a fiber content of 4.5‰, and a fiber length of 20 mm.

These results indicate that the relative significance of the influencing factors varied among different crack characteristic indicators; however, fiber length consistently exerted the least influence on the crack indicators, which is consistent with the findings reported by Hao [23] and Tang [26]. Notably, for the composite amended expansive soil prepared with 10% biochar, 4.5‰ fiber content, and 20 mm fiber length, all crack characteristic indicators were reduced to zero, indicating that no visible cracks developed in the composite amended specimen during the drying process. Nevertheless, a peripheral gap was observed between the specimen boundary and the mold, which was attributed to the overall shrinkage of the soil specimen.

3.3. Microstructural Analysis

SEM analysis was conducted on the improved soil specimens to examine their microstructural characteristics and elucidate the underlying improvement mechanisms.

Figure 11a presents a scanning electron micrograph of the biochar-amended soil at 1000× magnification. The expansive soil matrix predominantly exhibited a "turbulent structure," with the soil skeleton composed largely of aggregates formed by layered or flaky structures and colloidal components. A limited number of biochar particles were dispersed discretely throughout the soil, displaying morphologies resembling "honeycomb briquettes" and "blades." These particles contained abundant internal micropores and mesopores capable of absorbing and storing water through capillary action and releasing it gradually during drying, thereby buffering the shrinkage induced by water loss. This moisture buffering mechanism was corroborated by macroscopic observations: as the biochar content increased from 4% to 10%, the crack ratio decreased from 1.49% to 0.24%—a reduction of 86.8%—demonstrating a clear negative correlation and confirming that the pore structure of biochar constitutes the primary mechanism responsible for inhibiting desiccation cracking.



(**a**) (**b**)

Figure 11. Scanning electron micrographs. (**a**) Biochar improvement 1000×; (**b**) Sisal fiber improvement 105×.

Figure 11b shows a scanning electron micrograph of the sisal fiber-amended soil at 105× magnification. The sisal fibers appeared as elongated strips with rough surfaces characterized by distinct longitudinal textures. This surface morphology enhanced the friction coefficient at the fiber–soil interface, enabling the fibers to transfer tensile loads to the surrounding soil through interfacial shear stress. The fibers were intimately embedded within the soil matrix and formed an interwoven three-dimensional network, with no visible agglomeration or interfacial cracks. When a local shrinkage tendency developed, this network redistributed the stress to the surrounding regions through the pull-out resistance of the fibers, thereby mitigating stress concentration and preventing brittle failure. The macroscopic evidence supported these microstructural findings: as the fiber content increased from 1.5‰ to 6‰, the cohesion rose from 4.7 kPa to 50.3 kPa—a 970% increase—

confirming that fiber–soil interface friction and the three-dimensional network structure are the primary contributors to the cohesion enhancement.

Notably, the composite amended soil (10% biochar + 4.5‰ fiber + 20 mm) achieved complete suppression of visible cracks, an outcome that none of the single amendment methods attained. This synergistic effect demonstrates that the spatial complementarity between the rigid biochar skeleton and the flexible fiber network constitutes the microstructural basis for the combined improvement in crack resistance and mechanical strength.

4. Discussion

4.1. Analysis of Improvement Mechanism

The desiccation cracking mechanism of expansive soil is schematically illustrated in Figure 12a. Natural expansive soil is a three-phase system composed of soil particles, free water, and air. As the environmental humidity decreases, the free water between the surface soil particles evaporates first. Consequently, the soil particles undergo displacement and agglomerate into small units, progressively widening the gaps between adjacent aggregates. These gaps eventually evolve into cracks that continue to propagate into the deeper soil.

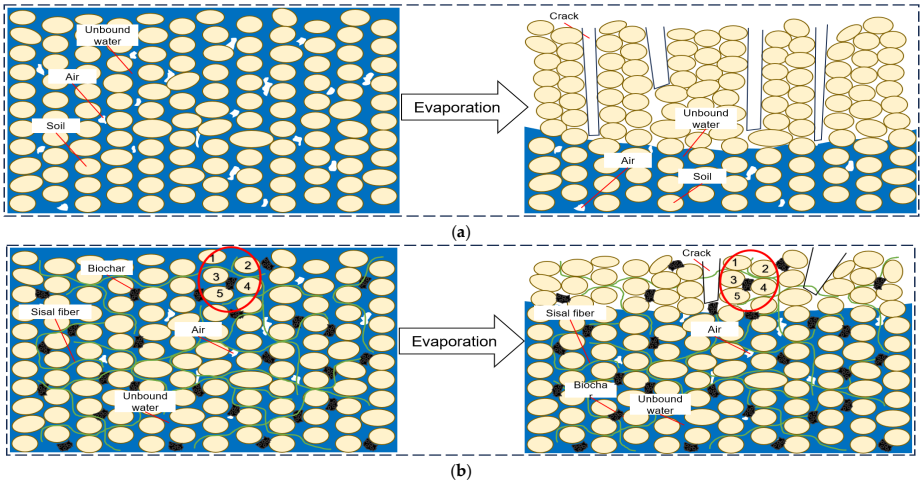


Figure 12. Schematic of desiccation cracking mechanisms for (**a**) natural expansive soil and (**b**) biochar-sisal fiber improved soil.

4.1.1. Influence of Biochar

The mechanism by which biochar suppresses soil cracking is illustrated in Figure 12b, with particular focus on the soil–biochar interaction within the highlighted red circle. When the soil loses water, the biochar particles maintain a constant volume, thereby immobilizing the adjacent soil particles (3, 4, and 5) and preventing their relative displacement. In contrast, soil particles 1 and 2, which lack direct contact with the biochar, migrate toward particles 3 and 4 as water evaporates. This differential movement manifests macroscopically as soil shrinkage and crack formation.

The inhibitory effect of biochar on cracking operates through two distinct mechanisms. The first is a moisture buffering effect arising from the abundant pore structure of biochar. When the soil is in a moist state, the pores absorb part of the free water through capillary action, thereby limiting the amount of water available for absorption by expansive clay minerals such as montmorillonite and consequently suppressing their swelling. As the environment becomes dry and the outer soil particles begin to lose water, the moisture retained within the biochar pores is gradually released through molecular diffusion, providing a compensating effect that retards the shrinkage of clay minerals [43]. A higher biochar content enables greater water storage and, in turn, a more pronounced compensating effect,

leading to more effective crack suppression. The second mechanism is a rigid skeleton effect attributable to the rough, angular surface morphology of biochar particles. These physical characteristics enable the biochar to restrict the relative displacement of adjacent soil particles through interlocking. With increasing biochar content, this restraining effect becomes more substantial, contributing not only to enhanced shear strength but also to the inhibition of crack initiation and propagation.

The inhibitory effect of biochar on the desiccation cracking of expansive soil can be primarily attributed to a moisture buffering effect. As the ambient humidity rises, the micropores and mesopores within the biochar absorb water through capillary action, thereby limiting the water available for absorption by clay minerals and suppressing their swelling. Conversely, under dry conditions, this stored water is gradually released via molecular diffusion, compensating for the water loss from the soil and retarding shrinkage [43]. This mechanism aligns with the findings of Zhao et al. [44], who demonstrated that biochar enhances the soil's water-holding capacity through its high porosity. In addition to this moisture regulation, the rigid skeleton effect of biochar further contributes to crack inhibition by restricting the relative displacement of soil particles through particle interlocking.

4.1.2. Influence of Sisal Fiber Content

The reinforcement mechanism of sisal fiber is schematically illustrated in Figure 12b. Sisal fibers possess rough surfaces and overlap with one another to form an irregular three-dimensional network, which substantially enhances the contact between the fibers and soil particles. This network contributes to crack suppression and strength improvement through two complementary mechanisms: interfacial friction enhancement and stress redistribution.

The first mechanism, interfacial friction enhancement, arises from the distinct longitudinal surface texture of the fibers, which increases the friction coefficient at the fiber–soil interface. This enables the fibers to more effectively convert tensile stresses into interfacial shear stresses [40]. The second mechanism, stress redistribution, operates when a local displacement tendency develops in the soil. The randomly distributed fiber network transmits stress from the affected region to the surrounding undisturbed soil through the pull-out resistance of the fibers, thereby homogenizing the stress distribution and preventing brittle failure due to localized stress concentration [45]. As the fiber content increases, the contact relationships among soil skeleton particles are progressively altered [40], enabling the amended soil to withstand higher normal and shear stresses. Simultaneously, the binding effect exerted by the fiber network on the surface soil particles becomes more pronounced, further restricting particle displacement and resulting in a significant reduction in crack area, mean crack width, and crack ratio.

This dual mechanism is consistent with the findings of Huang et al. [33] for glass fiber-reinforced expansive soil. Notably, the enhancement of soil integrity by fiber reinforcement is primarily manifested as a substantial increase in cohesion—which rose from 4.7 kPa to 50.3 kPa in this study, representing a 970% increase—rather than a change in the internal friction angle.

4.1.3. Influence of Sisal Fiber Length

The progressive decrease in the shear strength of expansive soil with increasing sisal fiber length can be primarily attributed to the reduction in the number of individual fibers at a fixed fiber content. Longer fibers result in a sparser spatial distribution, leaving certain regions of the soil without effective fiber reinforcement. These unreinforced regions are susceptible to premature failure under loading, thereby compromising the overall shear strength of the soil.

4.1.4. Synergistic Mechanism of Biochar and Sisal Fiber

The synergistic improvement of expansive soil by biochar and sisal fiber can be understood through three complementary aspects: mechanical complementarity, functional complementarity, and spatial scale complementarity.

Mechanically, biochar particles, characterized by high hardness and distinct angularity, form a rigid skeleton within the soil that primarily increases the internal friction angle (from 14.84° to 18.52°) through particle interlocking, thereby enhancing the shear resistance under compression. In contrast, sisal fibers, with their rough-surfaced fiber bundles, form a flexible three-dimensional network that significantly increases the cohesion (from 4.7 kPa to 50.3 kPa) through interfacial friction and interlocking, thereby enhancing the deformation resistance under tension. Together, these two materials establish a complementary reinforcement system that combines rigidity and flexibility: the rigid biochar skeleton provides structural support, while the flexible fiber network offers deformation restraint.

Functionally, the pore structure of biochar exerts a moisture buffering effect during wetting–drying cycles: it absorbs and stores part of the free water during wetting, thereby reducing the swelling of clay minerals, and slowly releases the retained water during drying, thereby delaying soil shrinkage [43]. This mechanism fundamentally reduces the swell–shrink amplitude of the expansive soil, thereby lowering the confining load that the fiber network must bear. On this basis, the three-dimensional fiber network further restrains the residual displacement of soil particles, promoting a more uniform stress distribution and effectively inhibiting crack formation [45]. The optimal combination of these two functional mechanisms—achieved at a biochar content of 10%, a sisal fiber content of 4.5‰, and a fiber length of 20 mm—resulted in the complete suppression of visible cracks on the specimen surface.

Spatially, biochar and sisal fibers operate at distinct scales. Biochar is distributed as discrete particles within the soil pores, typically at the micrometer to millimeter scale, where it fills small-sized voids and provides particle-level reinforcement. Sisal fibers, by contrast, form a continuous network that wraps around soil particles at the centimeter scale, offering macro-scale reinforcement and confinement. This spatial scale complementarity enables the soil to be simultaneously enhanced at both the microstructural and macrostructural levels, contributing to the overall improvement in mechanical performance and crack resistance.

4.2. Influence Mechanism of Biochar Pore Structure on Soil Behavior

The improvement in the desiccation cracking resistance and shear strength of expansive soil conferred by biochar is fundamentally rooted in its distinctive pore structure characteristics. The woody biochar employed in this study possesses a specific surface area of 209.14 m^2/g and contains abundant internal micropores and mesopores, which fulfill a dual function within the soil matrix. Under moist conditions, these pores absorb excess water through capillary action, thereby limiting the water available for absorption by expansive clay minerals such as montmorillonite and consequently suppressing their swelling. As the environment transitions toward dry conditions, the stored water is gradually released via molecular diffusion, exerting a buffering and compensating effect that retards shrinkage induced by water loss. This moisture regulation mechanism directly inhibits the initiation and propagation of desiccation cracks: as the biochar content increased from 4% to 10%, the crack ratio decreased by 86.8%. In addition to this pore-mediated effect, the biochar particles—characterized by high hardness and irregular morphology—form a discrete rigid skeleton within the soil. Under vertical loading, particle interlocking between the biochar and the surrounding soil particles occurs [38], leading to an increase in the internal friction angle from 14.84° to 18.52°, which constitutes the primary mechanism responsible for the enhanced shear strength. It should be noted that the above interpretation is derived from

SEM morphological observations and macroscopic mechanical trends; the dynamic process of water migration within the biochar pores remains to be verified through advanced techniques such as nuclear magnetic resonance.

4.3. Reinforcement Mechanism and Length Effect of Sisal Fiber

The reinforcement effect of sisal fiber on expansive soil can be understood from two perspectives: interface mechanics and spatial confinement. The fiber surface is distinctly rough (Figure 12b), giving rise to significant static friction and interlocking forces at the fiber–soil interface. When a displacement tendency develops within the soil, these interfacial forces enable the fibers to transfer local stress to the surrounding undisturbed regions, thereby homogenizing the stress distribution and preventing brittle failure induced by stress concentration. Macroscopically, this mechanism is reflected in a substantial increase in cohesion—from 4.7 kPa to 50.3 kPa as the fiber content increased from 1.5‰ to 6‰, representing a 970% increase.

An optimal fiber length exists for soil reinforcement, governed by the balance between the interfacial shear strength at the fiber–soil boundary and the tensile strength of the fiber itself. When the fiber length falls below the critical value, the fibers are prone to pull-out without fully mobilizing their intrinsic tensile capacity. Conversely, excessively long fibers are difficult to disperse uniformly and tend to entangle into clusters [24], creating weak planes around these agglomerations that lead to an 11–21% reduction in shear strength. This interpretation is consistent with the observations of Prabakar et al. [37] and provides a mechanical rationale for the peak cohesion of 29.7 kPa attained at a fiber length of 20 mm in the present study.

4.4. Comparison with Existing Studies

Comparison with recent international studies further validates the effectiveness of the combined biochar–fiber improvement approach. Ma et al. [46] reported that the addition of 8% biochar and 0.3% bagasse fiber to expansive soil from Chongzuo, Guangxi, reduced the linear shrinkage ratio from 11.1% to 3.2%, corresponding to a 71.2% reduction. In the present study, the combination of 10% biochar and 4.5‰ sisal fiber achieved complete elimination of visible cracks, yielding a more pronounced suppression effect. This superior performance may be attributed to the longer fiber length (20 mm) adopted herein, which is more conducive to forming a continuous three-dimensional network. Chen et al. [8] employed a combined improvement strategy using jute fiber, nylon fiber, and cement, reporting a 1380% increase in unconfined compressive strength at a fiber content of 0.5%. In contrast, the present study achieved complete crack suppression using purely natural materials—biochar and sisal fiber—without any cement addition, demonstrating that the synergistic effect of natural materials holds considerable potential to replace traditional cementitious binders. The RSM analysis conducted by Chen et al. [9] indicated that fiber content exerted a greater influence on compressive strength than biochar content. Conversely, the range analysis performed in this study (Table 5) revealed that biochar content had the greatest influence on crack length and crack ratio, whereas fiber content most strongly governed crack width. This apparent discrepancy likely arises from differences in the evaluation indicators employed and warrants further investigation. Hao et al. [23] demonstrated through wetting–drying cycle tests that sisal fiber reinforcement reduced the crack ratio and mean crack width by up to approximately one-half relative to the unreinforced soil. They further observed that the fibers increased the permeability coefficient of the expansive soil to approximately 2.4 times that of the unreinforced soil, thereby promoting more uniform water distribution and inhibiting crack widening. This mechanism aligns well with the three-dimensional fiber network structure observed by SEM in the

present study, providing corroborative evidence for the proposed mechanism that fibers suppress cracking through interfacial friction and stress redistribution. Additionally, Hao et al. [23] found that sisal fibers primarily restricted crack development in the vertical direction, resulting in only shallow surface cracks rather than penetrating fissures. This finding explains the observation in the present study that, although the composite amended soil completely suppressed visible surface cracks, an overall shrinkage gap between the specimen boundary and the mold remained.

It should be acknowledged that the above comparison is primarily conducted at the effect level, and the synergistic effect has not been rigorously quantified. This represents a notable limitation of the present study, particularly when compared with existing investigations that have employed quantitative methods such as RSM analysis.

4.5. Research Limitations and Future Work

Several limitations of the present study should be noted. Replicate tests were not conducted; consequently, standard deviations and statistical significance tests could not be provided. This limitation arose primarily from practical constraints: both the direct shear tests and desiccation cracking tests were time-intensive—each desiccation test required approximately 72 h—and the specimen preparation procedures were inherently complex. Nevertheless, the trends in strength and crack parameters with varying amendment contents were monotonic and well-defined, and exhibited strong consistency with patterns reported in the literature, confirming the reliability and regularity of the experimental results. Future research should incorporate a greater number of replicates and employ statistical methods such as analysis of variance (ANOVA) to rigorously assess the significance of the observed differences.

Beyond statistical rigor, future investigations should incorporate micromechanical testing to quantify the fiber–soil interface strength and to evaluate the specific contribution of biochar particles to the soil skeleton. Full factorial experimental designs should be adopted, and the synergistic effect should be quantified using an appropriate synergy factor formulation. Furthermore, the integration of single-fiber pull-out tests with X-ray micro-computed tomography (micro-CT) is strongly recommended, as this combined approach would enable direct measurement of the fiber–soil interface strength and three-dimensional visualization of the spatial distribution of biochar particles within the soil matrix, thereby providing the quantitative evidence required to substantiate the proposed synergistic mechanism.

4.6. Engineering Application Value and Recommendations

The biochar and sisal fiber employed in this study are both renewable, low-cost green materials with distinct raw material advantages, particularly in major sisal-producing regions such as Guangxi. Based on the experimental findings, the following engineering application recommendations are proposed. The optimal mix proportion—10% biochar, 4.5‰ sisal fiber, and a fiber length of 20 mm—completely suppressed visible crack formation during drying while significantly enhancing the shear strength relative to the plain soil. This proportion is well suited for subgrade filling, slope protection, and shallow foundation improvement.

Compared with traditional cement- and lime-based stabilization methods, the composite improvement scheme developed in this study offers several environmental and practical advantages. First, both components are environmentally friendly: biochar is derived from waste wood pyrolysis, and sisal fiber is a natural plant fiber; both are carbon-neutral materials, aligning with the principles of green geotechnical engineering. Second, locally available materials can be utilized—Guangxi is the principal sisal-producing region in China, and

biochar can be produced from indigenous agricultural waste—thereby substantially reducing material transportation costs. Third, the scheme eliminates the need for cementitious binders entirely, as complete suppression of desiccation cracking was achieved without cement addition, avoiding the high carbon emissions inherent to cement production.

During construction, achieving uniform fiber dispersion within the soil matrix is critical to realizing the designed performance. Mechanical mixing is strongly recommended to ensure homogeneous fiber distribution and to prevent fiber entanglement and clumping. The compaction degree of the improved soil should be controlled at approximately 94%: excessive compaction may induce fiber breakage, whereas insufficient compaction may impede the formation of an effective three-dimensional fiber network.

5. Conclusions

This study investigated the individual and combined effects of biochar and sisal fiber on the shear strength and crack characteristics of expansive soil. The main conclusions are summarized as follows:

The shear strength of expansive soil can be enhanced by the individual addition of either biochar or sisal fiber, with the strength increasing progressively at higher amendment contents. However, the shear strength decreases with increasing sisal fiber length.

Biochar and sisal fiber exert contrasting effects on the shear strength parameters. Increasing the biochar content raises the internal friction angle but reduces the cohesion, whereas increasing the sisal fiber content substantially enhances the cohesion, accompanied by a moderate reduction in the internal friction angle. As the fiber length increases, the cohesion first increases and then decreases, while the internal friction angle follows an opposite trend.

Both biochar and sisal fiber, when applied individually, effectively inhibit crack development in expansive soil, with all crack indicators decreasing progressively at higher amendment contents. At a biochar content of 10%, the crack length, crack width, and crack ratio are reduced by 69.7%, 56.1%, and 86.8%, respectively, relative to the plain soil. At a sisal fiber content of 6‰, the corresponding reductions are 49%, 46.1%, and 72.4%.

For the composite amended soil, the factors influencing crack length and crack ratio follow the order: biochar content > fiber content > fiber length, whereas the order for crack width is fiber content > biochar content > fiber length. Under the optimal combination of 10% biochar, 4.5‰ sisal fiber, and a fiber length of 20 mm, no visible cracks are observed on the specimen surface after drying.

Microstructural analysis reveals that biochar particles possess rough surfaces and blade-like edges, with platy soil particles filling the coarse pores within the biochar. Sisal fibers exhibit distinct longitudinal surface textures and are non-directionally interwoven throughout the soil matrix. The synergistic interaction between the rigid biochar skeleton and the flexible fiber network contributes to the significant improvement in both the mechanical strength and crack resistance of the expansive soil.

Although both biochar and sisal fiber are renewable, low-cost green materials with distinct raw material advantages in major sisal-producing regions such as Guangxi, and the optimal mix proportion identified herein is suitable for subgrade filling, slope protection, and shallow foundation improvement, this study has certain limitations. Specifically, long-term durability tests—evaluating performance degradation after multiple wetting–drying cycles—and field-scale verification were not conducted. Future research should therefore focus on the long-term service performance and life-cycle economic analysis of the composite amended soil under field conditions.

Author Contributions: Y.L.: Writing—editing & translation, funding acquisition. Y.Z.: Writing—review & editing. A.C.: Supervision, Resources, Conceptualization. L.L.: Writing—original draft, Visualization, Validation, Investigation, Formal analysis. All authors have read and agreed to the published version of the manuscript.

Funding: This research was funded by Guangxi Science and Technology Department grant number 20243041 and the Innovation Project of Guangxi Graduate Education YCSW2025334.

Data Availability Statement: The original contributions presented in this study are included in the article. Further inquiries can be directed to the corresponding author.

Acknowledgments: The authors sincerely acknowledge the support provided by the Nanning Science and Technology Plan Project No. 20243041 (Research and Industrial Application of Fluidized Recycled Materials from Engineering Spoil) and the Innovation Project of Guangxi Graduate Education YCSW2025334 (A study on the mechanical properties of early strength fluidized clay) during the research process.

Conflicts of Interest: The authors declare no conflicts of interest.

References

1. Shi, B.; Jiang, H.T.; Liu, Z.B.; Fang, H.Y. Engineering geological characteristics of expansive soils in China. *Eng. Geol.* **2002**, *67*, 63–71. [CrossRef]
2. Kong, L.W.; Zeng, Z.X.; Bai, W.; Wang, M. Engineering geological properties of weathered swelling mudstones and their effects on the landslides occurrence in the Yanji section of the Jilin-Hunchun high-speed railway. *Bull. Eng. Geol. Environ.* **2018**, *77*, 1491–1503.
3. Ozer, M.; Ulusay, R.; Isik, N.S. Evaluation of damage to light structures erected on a fill material rich in expansive soil. *Bull. Eng. Geol. Environ.* **2012**, *71*, 21–36.
4. Liu, J.J.; Yu, J.H.; Hu, S.S.; Hu, C.L.; Wang, J.J.; Yu, Z.W.; Huang, K. Analysis of crack evolution of expansive soil embankment under extreme arid climate. *Case Stud. Constr. Mater.* **2024**, *20*, e02902. [CrossRef]
5. Cai, Z.L.; Cheng, Q.; Tang, C.S.; Ji, X.L.; Xu, J.J.; Gu, Y.D.; Shi, B. Size effects of desiccation cracking behavior in clayey soil. *Acta Geotech.* **2026**, *21*, 2273–2289.
6. Murugesan, S.; Rajesh, S.; Abuel-Nagab, H.M. Crack-hydro-deformation analysis of expansive soil: Implications on heave–subsidence response. *Can. Geotech. J.* 2026, *in press*. [CrossRef]
7. Jiang, M.J.; Wang, M.; Huang, Y.L.; Jia, Y.K.; Garg, A.; Mei, G.X. Biochar stabilises vegetated expansive slopes by way of moisture and temperature regulation. *Environ. Geotech.* **2025**, 2500092. [CrossRef]
8. Chen, H.; Zhu, J.Z.; Du, H.; Wang, Q.; Wang, W.H.; Wang, B.X.; Gao, X.; Ding, Q. Enhancement of micro-mechanical characteristics of expansive soil through synergistic incorporation of jute and nylon fibers with cement. *Results Eng.* **2025**, *26*, 104567. [CrossRef]
9. Chen, A.J.; Chen, F.Y.; Ding, C.Y.; Shi, X. Effect of biochar and sisal fiber on compressive strength of expansive soil. *Case Stud. Constr. Mater.* **2025**, *23*, e05071. [CrossRef]
10. Lehmann, J.; Gaunt, J.; Rondon, M. Bio-char sequestration in terrestrial ecosystems—A review. *Mitig. Adapt. Strateg. Glob. Change* **2006**, *11*, 403–427. [CrossRef]
11. Vu, T.M.; Doan, D.P.; Van, H.T.; Nguyen, T.V.; Vigneswaran, S.; Ngo, H.H. Removing ammonium from water using modified corncob biochar. *Sci. Total Environ.* **2017**, *579*, 612–619. [CrossRef] [PubMed]
12. Ahmed, M.B.; Zhou, J.L.; Ngo, H.H.; Johir, M.A.H.; Sornalingam, K. Sorptive removal of phenolic endocrine disruptors by functionalized biochar: Competitive interaction mechanism, removal efficacy and application in wastewater. *Chem. Eng. J.* **2018**, *335*, 801–811. [CrossRef]
13. Wu, S.; He, H.; Inthapanya, X.; Yang, C.; Lu, L.; Zeng, G.; Han, Z. Role of biochar on composting of organic wastes and remediation of contaminated soils—A review. *Environ. Sci. Pollut. Res.* **2017**, *24*, 16560–16577. [CrossRef]
14. Chemerys, V.; Baltrėnaitė, E. Influence of intrinsic properties of lignocellulosic feedstock on adsorptive properties of biochar. *J. Environ. Eng.* **2018**, *144*, 04018075. [CrossRef]
15. Kumar, H.; Cai, W.; Lai, J.; Chen, P.; Ganesan, S.P.; Bordoloi, S.; Liu, X.; Wen, Y.P.; Garg, A.; Mei, G. Influence of in-house produced biochars on cracks and retained water during drying-wetting cycles: Comparison between conventional plant, animal, and nano-biochars. *J. Soils Sediments* **2020**, *20*, 1983–1996. [CrossRef]
16. Zhang, D.; Lv, Q.; Xu, X.; Li, Y.; Liu, Y.; Yang, J. Effect of Corn Stalk Biochar on the Evolution of Water Evaporation and Cracking of Soil. *Geofluids* **2022**, *2022*, 5703377. [CrossRef]

17. Lu, Y.; Gu, K.; Zhang, Y.; Tang, C.S.; Shen, Z.; Shi, B. Impact of biochar on the desiccation cracking behavior of silty clay and its mechanisms. *Sci. Total Environ.* **2021**, *794*, 148608. [CrossRef] [PubMed]
18. Yang, B.; Xu, K.; Zhang, Z. Mitigating evaporation and desiccation cracks in soil with the sustainable material biochar. *Soil Sci. Soc. Am. J.* **2020**, *84*, 461–471. [CrossRef]
19. Zong, Y.; Chen, D.; Lu, S. Impact of biochars on swell–shrinkage behavior, mechanical strength, and surface cracking of clayey soil. *J. Plant Nutr. Soil Sci.* **2014**, *177*, 920–926. [CrossRef]
20. Wang, H.; Garg, A.; Huang, S.; Mei, G. Mechanism of compacted biochar-amended expansive clay subjected to drying–wetting cycles: Simultaneous investigation of hydraulic and mechanical properties. *Acta Geophys.* **2020**, *68*, 1625–1638. [CrossRef]
21. Yadav, S.K.; Bag, R. Influence of prolong curing, freeze thaw cycles on strength and compaction condition on water retention behaviour of bamboo biochar amended soils. *Sci. Rep.* **2025**, *15*, 9. [CrossRef] [PubMed]
22. Qiang, X.; Lu, H.J.; Li, Z.Z.; Liu, L. Cracking, water permeability and deformation of compacted clay liners improved by straw fiber. *Eng. Geol.* **2014**, *178*, 82–90. [CrossRef]
23. Hao, J.B.; Li, G.C.; Liu, Z.Y.; Cui, F.Q.; Jiang, Z.W. Anti-cracking Mechanism of Sisal Fiber-reinforced Expansive Soil under Dry-wet Cycle and Its Influencing Factors. *J. Hunan Univ. (Nat. Sci.)* **2024**, *51*, 147–158.
24. Chaduvula, U.; Viswanadham, B.V.S.; Kodikara, J. A study on desiccation cracking behavior of polyester fiber-reinforced expansive clay. *Appl. Clay Sci.* **2017**, *142*, 163–172. [CrossRef]
25. El Hajjar, A.; Ouahbi, T.; Taibi, S.; Eid, J.; Hattab, M.; Fleureau, J.M. Assessing crack initiation and propagation in flax fiber reinforced clay subjected to desiccation. *Constr. Build. Mater.* **2021**, *278*, 122392. [CrossRef]
26. Tang, C.S.; Shi, B.; Cui, Y.J.; Liu, C.; Gu, K. Desiccation cracking behavior of polypropylene fiber–reinforced clayey soil. *Can. Geotech. J.* **2012**, *49*, 1088–1101. [CrossRef]
27. Huang, F.R.; Fang, Y.R.; Tan, M.J.; Wang, Z.; Li, J.; Wang, L.; Guo, H. Experimental Study on Dry Shrinkage Cracks of Expansive Soil Modified by Polypropylene Fiber. *Bull. Geol. Sci. Technol.* **2023**, *37*, 461–464.
28. Su, L.X.; Lei, Y.; Liu, X.; Wang, Y.; Zhang, L. Study on the Fracture Characteristics of Fiber-Amended Swelling Soil under Dry and Wet Cycles. *Non-Met. Mines* **2023**, *46*, 32–35.
29. Han, C.P.; Tian, J.Y.; Zhang, J.; Li, J.H. Analysis of crack characteristics of fiber-reinforced expansive soil under wetting-drying cycle. *J. Jilin Univ. (Eng. Technol. Ed.)* **2019**, *49*, 392–400.
30. Xiao, G.Y.; Wang, H.P.; Deng, J.; Liu, X.; Yang, S. Sodium silicate solution and polypropylene fiber modified expansive soil strength and crack characteristics. *J. Railw. Sci. Eng.* **2025**, *22*, 1074–1086.
31. Song, K.; Liu, Y.; Ruan, D.; Huang, W.; Yuan, J.J.; Ai, D. Strength and cracking behavior of weak expansive soil improved by basalt fiber. *Bull. Geol. Sci. Technol.* **2026**, *45*, 110–120.
32. Huang, Z.; Sun, H.Y.; Dai, Y.M.; Hou, P.B.; Zhou, W.Z.; Bian, L.L. A study on the shear strength and dry-wet cracking behaviour of waste fibre-reinforced expansive soil. *Case Stud. Constr. Mater.* **2022**, *16*, e01142.
33. Bordoloi, S.; Garg, A.; Sreedeep, S.; Lin, P.; Mei, G. Investigation of cracking and water availability of soil-biochar composite synthesized from invasive weed water hyacinth. *Bioresour. Technol.* **2019**, *285*, 121321.
34. *GB/T 50123–2019*; Standard for Geotechnical Testing Method. China Planning Press: Beijing, China, 2019. Available online: https://openstd.samr.gov.cn/bzgk/gb/std_gb?gbNo=GB/T%2050123-2019 (accessed on 9 May 2026).
35. Liu, D.; Sun, W.; Kong, Y.; Wang, H.; Zhang, X. Effect of dry and wet cycles on the strength characteristics of biochar–clay mixture. *Processes* **2023**, *11*, 970. [CrossRef]
36. Shukla, A.K.; Sharma, A.K. Influence of biochar in the calcite precipitation of sandy soil using *Sporosarcina ureae*. *J. Environ. Manag.* **2024**, *359*, 121048. [CrossRef]
37. Prabakar, J.; Sridhar, R.S. Effect of random inclusion of sisal fibre on strength behaviour of soil. *Constr. Build. Mater.* **2002**, *16*, 123–131. [CrossRef]
38. Sadasivam, B.Y.; Reddy, K.R. Engineering properties of waste wood-derived biochars and biochar-amended soils. *Int. J. Geotech. Eng.* **2015**, *9*, 521–535. [CrossRef]
39. Hussain, R.; Bordoloi, S.; Gupta, P.; Garg, A.; Ravi, K.; Sreedeep, S.; Sahoo, L. Investigating biochar-amended soil as a potential lightweight material for embankments. *Ecol. Eng.* **2022**, *180*, 106645. [CrossRef]
40. Jiang, R.; Wang, J.; Xiao, T.; Zhang, D. Effect of sisal fibers on the disintegration characteristics of sisal fiber-amended loess. *Constr. Build. Mater.* **2024**, *453*, 139032. [CrossRef]
41. Zhang, Y.; Gu, K.; Li, J.; Tang, C.S.; Shen, Z.; Shi, B. Effect of biochar on desiccation cracking characteristics of clayey soils. *Geoderma* **2020**, *364*, 114182. [CrossRef]
42. Wang, X.; Gu, K.; Zhang, Y.; Lu, Y.; Tang, C.S.; Shi, B. Effects of biochar on desiccation cracking characteristics of different soils. *Chin. J. Geotech. Eng.* **2023**, *45*, 876–882.
43. An, Y.; Lu, J.; Niu, R.; Li, M.; Zhao, X.; Huang, X.; Huang, H.; Garg, A.; Zhussupbekov, A. Exploring effects of novel chemical modification of biochar on soil water retention and crack suppression: Towards commercialization of production of biochar for soil remediation. *Biomass Convers. Biorefinery* **2023**, *13*, 13897–13910.

44. Zhao, Y.; Liu, Z.; Song, J.; Cheng, K.; Yang, F. Improvement of Soil Physical, Chemical, and Biological Properties by Waste-derived Biochar. In *Waste-Derived Biochar for Sustainable Rural Revitalization*; Sun, Y., Tsang, D.C.W., Eds.; Wiley: Hoboken, NJ, USA, 2025.
45. Hao, J.B.; Zhang, H.; Li, G.C.; Liu, Z.Y.; Huang, J.X.; Jiang, Z.W. Strength and cracking characteristics of expansive soil improved by fly ash and sisal fiber. *J. Railw. Sci. Eng.* **2022**, *19*, 2620–2628. [CrossRef]
46. Ma, S.K.; Yue, H.; He, B.F.; Liao, L.P.; Shao, Y. Engineering Properties and Microscopic Mechanism of Expansive Soils Improved by Biochar and Bagasse Fibers. *J. Mater. Civ. Eng.* **2025**, *37*, 04025098. [CrossRef]

Disclaimer/Publisher's Note: The statements, opinions and data contained in all publications are solely those of the individual author(s) and contributor(s) and not of MDPI and/or the editor(s). MDPI and/or the editor(s) disclaim responsibility for any injury to people or property resulting from any ideas, methods, instructions or products referred to in the content.